PHYSICAL REVIEW B, VOLUME 63, 064404

Effects of phase separation on the magnetization, x-ray diffraction, and Raman scattering of $(La_{1-y}Nd_y)_{1-x}Ca_xMnO_3$ $(y=0,0.5,1.0; x=\frac{1}{3})$

E. Granado,* A. García, J. A. Sanjurjo, C. Rettori, and I. Torriani

Instituto de Física ''Gleb Wataghin,'' UNICAMP, 13083-970, Campinas-SP, Brazil

(Received 9 June 2000; revised manuscript received 25 September 2000; published 18 January 2001)

Dc-magnetization, x-ray diffraction, and Raman-scattering studies in polycrystalline $(La_{1-y}Nd_y)_{1-x}Ca_xMnO_3$ ($y=0.0,0.5,1.0$, and $x=1/3$) samples are presented. The samples with $y=0.5$ and 1.0 show complex magnetic states at low temperatures, with a ferromagnetic coupling strength that weakens with increasing y. X-ray measurements show a single crystallographic phase at all temperatures for $y=0.5$, with lattice parameter anomalies at temperatures related to electronic and magnetic transitions. The presence of high-frequency vibrational modes in Raman-scattering measurements indicates the existence of charge- and orbital-ordered domains for $y=0.5$ and 1.0, which are closely related to the antiferromagnetic component identified by the magnetization experiments. The close relationship between results obtained by magnetic, structural, and optical probes is discussed.

DOI: 10.1103/PhysRevB.63.064404 PACS number(s): 75.50.−y, 78.30.−j, 63.20.−e, 61.10.−i

I. INTRODUCTION

In the last few years many studies on doped manganese perovskites $(R_{1-y}R'_y)^{3+}_{1-x}A^{2+}_xMnO_{3+\delta}$ (R,R'=La, rare earths; A=Ca,Sr,Ba) have revealed a rich variety of new physical phenomena, among them, a colossal magnetoresistance for some compositions. One of the key properties of these systems is the tendency of the carriers to form charge- and orbital-ordered Mn e_g states (CO and OO, respectively). This was invoked to understand the rather complex spin alignment observed in $La_{1/2}Ca_{1/2}MnO_3$ (Refs. 1 and 2) and other half-doped manganites. Actually, high-resolution electron microscopy experiments detected an **a**- or **c**-axis doubling (*Pnma* setting) due to the OO of the Mn^{3+} e_g states,[3] confirming the existence of low-T CO and OO in $La_{1/2}Ca_{1/2}MnO_3$. The low-T Mn spin alignment in CO states is usually AFM, and compete with the double exchange (DE) ferromagnetic (FM) coupling. Such competition between AFM CO and FM charge delocalized (CD) states is likely responsible for the FM-antiferromagnetic (AFM) transition at $T_{FM\text{-}AFM}\sim 170$ K found in $La_{1/2}Ca_{1/2}MnO_3$.[4] It was shown that manganese perovskites with reduced FM coupling, obtained by decreasing the rare-earth-site mean radius with fixed doping rate,[5,6] present phase separation (PS), on a submicrometric scale, between CO and CD domains for $T\lesssim 200$ K.[7] Electronic PS on such a large length scale and temperature interval is an astonishing and unusual effect in solid state physics.[8] Due to the crystal atomic periodicity, PS between two competing physical states, each one with a different lattice configuration, must be accompanied by interface strains; therefore, the PS state may be more energetic than the pure states and might be not stable. The mechanisms that stabilize the PS state in the reduced-T_C manganites at low T are not fully understood. Particularly, it is not determined yet whether the submicrometric scale PS is favored by doping fluctuations throughout the sample in the same length scale or, alternatively, if this is an intrinsic phenomenon, driven by instabilities of both CO and CD single-phase configurations. These issues remain to be clarified by more detailed studies in reduced-T_C doped manganese perovskites.

The $(La_{1-y}Nd_y)_{1-x}Ca_xMnO_3$ series for $x\sim 1/3$ has been thoroughly studied,[9–16] and may be classified as a typical FM-coupling-controlled system of manganese perovskites. Systematic studies indicate that this system shows clear manifestation of PS in magnetization measurements for $y>0.4$.[16] Also, neutron-diffraction patterns of $La_{1/3}Nd_{1/3}Ca_{1/3}MnO_3$ ($y=0.5$) show a OO superstructure peak that strengths considerably below $T_{OO}\sim 210$ K.[14] An AFM extra peak was detected below $T_N\sim 170$ K and FM contributions to the nuclear Bragg peaks were observed below $T_C\sim 200$ K.[14] These neutron-diffraction results are also consistent with the PS proposed for the manganites with reduced FM coupling. In this work, we present magnetization, x-ray diffraction, and Raman-scattering studies in $(La_{1-y}Nd_y)_{2/3}Ca_{1/3}MnO_3$ at three distinct regimes: strong ($y=0.0$), average ($y=0.5$), and weak ($y=1.0$) FM coupling, with respect to the competing AFM interactions. By means of such a combination of experimental techniques and compositions, deeper insight into the magnetic, structural, and electronic properties of this complex family of compounds is obtained.

II. EXPERIMENTAL DETAILS

Polycrystalline ceramic samples were prepared by conventional solid-state reaction methods, sucessively heating stoichiometric mixtures of La_2O_3, Nd_2O_3, $CaCO_3$, and MnO_2 at 1200, 1350, and 1400 °C for 36 h with intermediate grindings. The powders were then pelletized and sintered at 1200 °C for 12 h. The structure and phase purity were checked by x-ray powder diffraction. Well resolved x-ray patterns were taken with Cu $K\alpha$ radiation (1.5415 Å) of a Rigaku conventional source and a high-resolution diffractometer with a low T attachment. Lattice parameters were obtained using a Rietveld refinement program.[17] dc-magnetization measurements were done in a Quantum Design Superconducting quantum interference device (SQUID) magnetometer, and M vs T curves were taken with a temperature variation rate of 0.5 K/min. In this work T_C

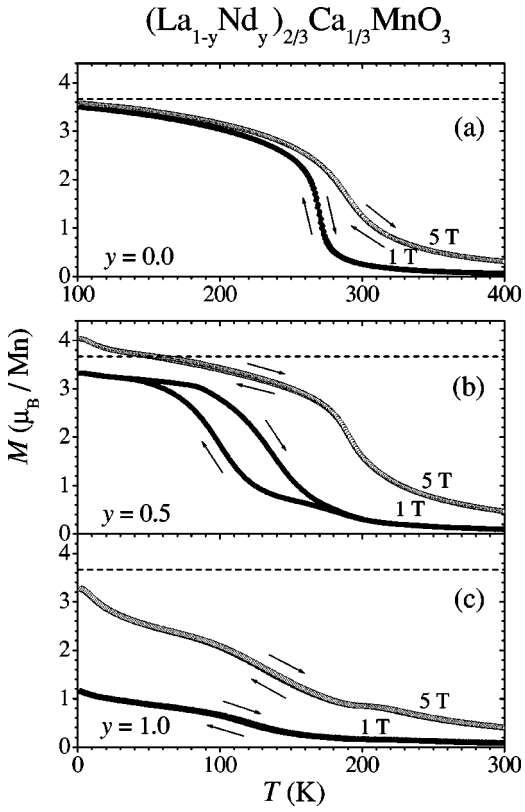

FIG. 1. M vs T curves for $(La_{1-y}Nd_y)_{2/3}Ca_{1/3}MnO_3$ polycrystalline samples with $y=0.0$ (a), $y=0.5$ (b), and $y=1.0$ (c), taken upon warming and cooling, for $H_{app}=1$ T (closed symbols) and $H_{app}=5$ T (open symbols).

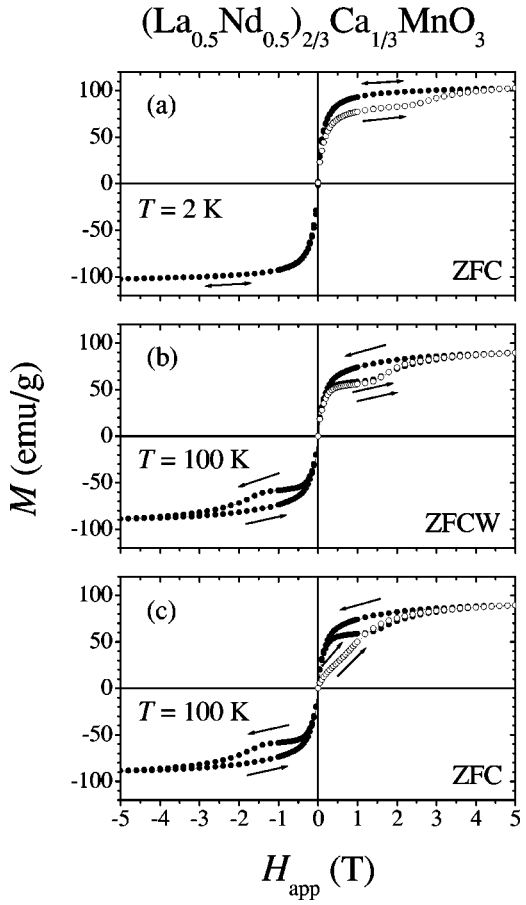

FIG. 2. M vs H hysteresis loops for $(La_{0.5}Nd_{0.5})_{2/3}Ca_{1/3}MnO_3$, taken at (a) $T=2$ K after zero field cooling (ZFC), (b) $T=100$ K after zero field cooling to 2 K and posterior zero field warming (ZFCW), and (c) $T=100$ K after ZFC. The open symbols indicate the first part of the loops, taken between 0 and 5 T, while the filled symbols accounts for the closed hysteresis circle, 5 T→−5 T→5 T.

was defined at the inflection points of the corresponding magnetization curves. Raman-scattering measurements were performed in a pseudobackscattering geometry using a Jobin Yvon T64000 triple spectrometer equipped with a charge-coupled device (CCD) camera. The samples were mounted on the cold finger end of a closed-cycle He refrigerator, and were excited with the 514.5 nm line of an argon ion laser, focused in a diameter of ~50 μm with incident laser power of less than 3 mW. T-dependent Raman measurements were performed upon heating the samples.

III. EXPERIMENTAL RESULTS

The $La_{2/3}Ca_{1/3}MnO_3$, $La_{1/3}Nd_{1/3}Ca_{1/3}MnO_3$, and $Nd_{2/3}Ca_{1/3}MnO_3$ samples will be termed $y=0.0$, $y=0.5$, and $y=1.0$ samples, respectively. Figures 1(a), 1(b) and 1(c) show, respectively, the T dependence of the dc-magnetization for the $y=0.0$, $y=0.5$, and $y=1.0$ samples taken with $H_{app}=1$ T and 5 T upon cooling and warming after field cooling. The saturation moment, expected for perfect FM alignment of Mn spins, is indicated by the dashed lines. For $y=0.0$, a sharp FM transition is observed at $T_C=265$ K for $H_{app}=1$ T. For $H_{app}=5$ T, the transition temperature is shifted to $T_C=285$ K. Within our experimental resolution (~1 K), no thermal hysteresis is observed for these samples. In contrast, for $y=0.5$ and $H_{app}=1$ T, the upturn of the FM component is significantly broader than that of $y=0.0$ [see Fig. 2(b)]. Besides, a large thermal hysteresis is observed, with $T_C^{Warm}\sim 120$ K and $T_C^{Cool}\sim 80$ K. However, for $H_{app}=5$ T, the shape of the magnetization curves near the FM transition are similar to those of the $y=0.0$ sample, with no thermal hysteresis, but with $T_C=180$ K. We attribute the low-T magnetization tail, above the FM saturation moment of Mn spins for $y=0.5$ and $H_{app}=5$ T, to an extra magnetization due to the Nd^{3+} ions. For $y=1.0$ and for $H_{app}=1$ T and 5 T, no thermal hysteresis is observed and the low-T magnetization is reduced.

Figure 2(a) shows the M vs H_{app} loop for the $y=0.5$ sample, taken at $T=2$ K after zero field cooling (ZFC). In the first part of the loop (open symbols), an increase of the saturation moment from ~80 emu/g to ~100 emu/g is observed for $H_{app}\gtrsim 2.5$ T. After this, the sample behaves as a conventional FM material (closed symbols) with saturation moment of ~100 emu/g. Figure 2(b) shows the M vs H_{app} loop for the same sample, at $T=100$ K. The sample was ZFC to 2 K and then warmed up under zero field to $T=100$ K (ZFCW). An increase of the FM moment, for $H_{app}\gtrsim 1.5$ T, is also observed. As the field decreases from 5 T to 0 T, the sample behaves as a conventional ferromagnet. However, as

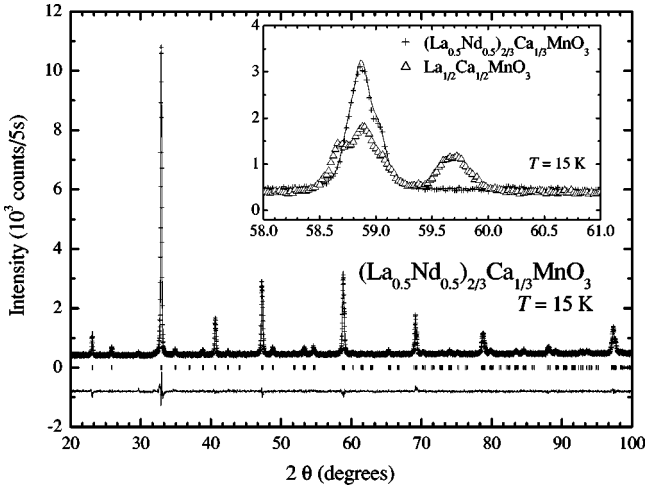

FIG. 3. Observed (symbols) and calculated (line) x-ray powder diffractograms at $T=15$ K for the $(La_{0.5}Nd_{0.5})_{2/3}Ca_{1/3}MnO_3$ sample. The difference between both diffractograms is also displayed. The inset shows, for a selected angular range, the observed and calculated profiles of $(La_{0.5}Nd_{0.5})_{2/3}Ca_{1/3}MnO_3$ and the observed profile of a $La_{1/2}Ca_{1/2}MnO_3$ sample at $T=15$ K.

an external field is applied in the opposite direction, a clear reduction of the FM saturation moment is again observed at low fields. Finally, the FM moment is increased again for $|H_{app}| \gtrsim 1.5$ T. Figure 2(c) shows the M vs H_{app} loop for the same sample and temperature of the Fig. 2(b), but with different thermal history. In this case, the sample was zero field cooled to $T=100$ K. The first part of the loop (open symbols) shows that the magnetization begins to saturate in ~ 30 emu/g, but the application of a field $H_{app} \gtrsim 0.5$ T increases the saturation moment. After the application of a field of 5 T, the M vs H_{app} loop at $T=100$ K is exactly the same as those taken under ZFCW conditions [see Fig. 2(b)]. For the $y=0.0$ sample, a typical FM loop is observed for $T=2$ K, with no field hysteresis (not shown). The M vs H_{app} curve for $y=1.0$ at low T is similar to that shown in Ref. 16, presenting a weak FM contribution (not shown).

Figure 3 shows the x-ray powder diffractogram at $T=15$ K for the $(La_{0.5}Nd_{0.5})_{2/3}Ca_{1/3}MnO_3$ sample, compared to a model profile generated after a Rietveld refinement performed under the assumption of a single crystallographic phase with $Pnma$ space group. The inset of Fig. 3 shows a selected region ($58° < 2\theta < 61°$) of the x-ray powder diffractograms of the $(La_{0.5}Nd_{0.5})_{2/3}Ca_{1/3}MnO_3$ and $La_{0.5}Ca_{0.5}MnO_3$ compounds at $T=15$ K. The latter compound presents a ''pure'' $x=0.5$ type CO and OO state at low T,[3,18] and also shows a large orthorhombic distortion of the lattice parameters (see inset of Fig. 3).[4] Within our experimental resolution, no evidence for the existence of other crystallographic phases in the $(La_{0.5}Nd_{0.5})_{2/3}Ca_{1/3}MnO_3$ sample (see Fig. 3), as well as in the $y=0.0$ and $y=1.0$ samples (not shown), was found at any temperature.

Figures 4(a) and 4(b) show the T evolution of the $Pnma$ orthorhombic lattice parameters and unit-cell volume for the $y=0.0$ and $y=0.5$ samples, respectively, taken upon cooling (open symbols) and warming (closed symbols). The FM onset temperature for both samples, taken from Fig. 1, as well

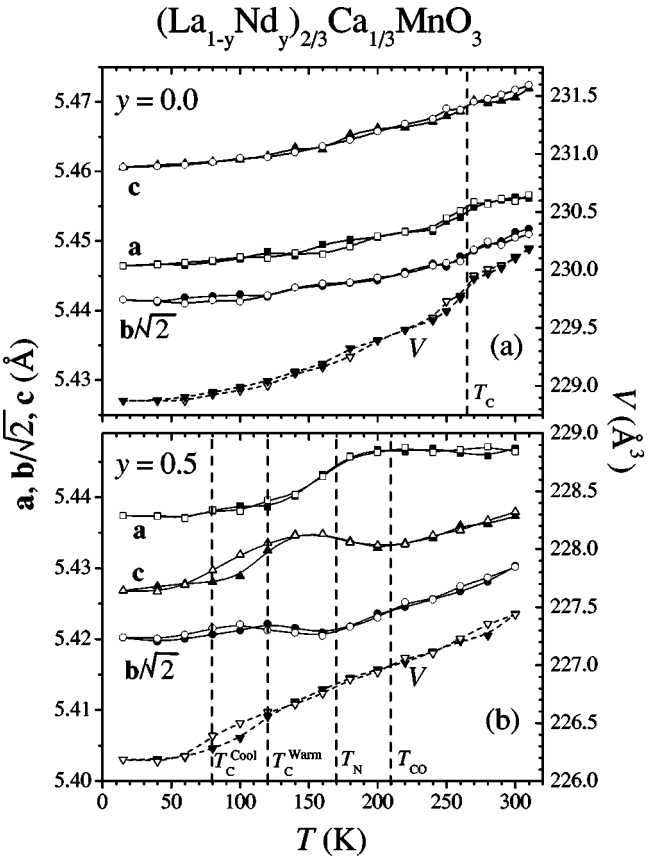

FIG. 4. T dependence of the **a**, **b**, and **c** lattice parameters and unit-cell volume for $La_{2/3}Ca_{1/3}MnO_3$ (a) and $La_{1/3}Nd_{1/3}Ca_{1/3}MnO_3$ (b), taken upon warming (closed symbols) and cooling (open symbols).

as the CO and AFM onset temperatures for $y=0.5$, taken from neutron-diffraction studies,[14] are indicated by dashed lines. For $y=0.0$, a unit-cell volume contraction is observed below $T_C=265$ K [see Fig. 4(a)], consistent with previous neutron-diffraction studies in this material.[19] Comparison of our results in Fig. 4(a) with neutron-diffraction data on the same material[19] and synchrotron x-ray diffraction data for $La_{0.75}Ca_{0.25}MnO_3$,[4] indicates that tube x-ray diffraction has enough resolution to study lattice parameter anomalies of the nearly-cubic orthorhombic manganites. For $y=0.5$, one observes the following features: (i) a change of the **a** and **c** lattice parameters behavior below $T \approx 200$ K, (ii) a change of behavior of the **b** and **c** lattice parameters below $T \approx 160$ K,[14] and (iii) a small volume contraction (0.05%) below $T_C^{Warm} \approx 120$ K (warming) and $T_C^{Cool} \approx 80$ K (cooling) [see Fig. 4(b)]. Notice that the features (i) and (ii) are not accompanied by unit-cell volume anomalies [see Fig. 4(b)].

The T evolution of the Raman spectra for the $y=0.0$, $y=0.5$, and $y=1.0$ samples are shown in Figs. 5(a), 5(b) and 5(c), respectively. For $y=0.0$ and $T=10$ K [see Fig. 5(a)], phonon peaks are observed at 67, 77, 139, ~ 200, 238, ~ 270, 415, and 438 cm^{-1}, as well as a weak and broad structure centered at ~ 680 cm^{-1}. This spectrum agrees with those previously reported for this compound,[20–22] and is also similar to the Raman spectrum of other FM orthorhombic

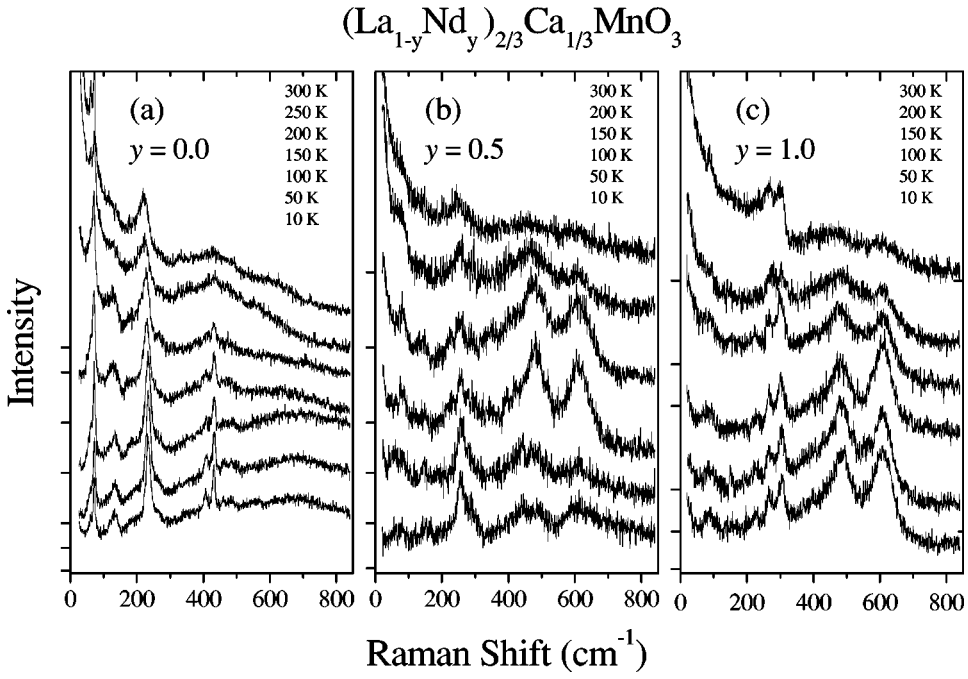

FIG. 5. Raman spectra, taken between 10 K and 300 K, for $(La_{1-y}Nd_y)_{2/3}Ca_{1/3}MnO_3$ ceramic samples with $y=0.0$ (a), $y=0.5$ (b), and $y=1.0$ (c).

and rhombohedral manganese perovskites.[23] As the temperature increases, a diffusive scattering is observed and becomes dominant near and above $T_C=265$ K. This diffusive contribution was observed in other doped manganites in the PM phase, and has been associated with carrier hopping processes.[24,25] In addition, two broad modes at ~ 480 and ~ 610 cm^{-1} are detected for $T \gtrsim T_C$ [see Fig. 5(a)], with an apparently lower relative intensity than those observed in the PM phase of $La_{0.7}Ca_{0.3}MnO_3$ thin films.[21] For $y=0.5$ [see Fig. 5(b)] and $T=10$ K, phonon peaks at 85, 145, 255, and ~ 290 cm^{-1}, and weak contributions from the ~ 480 and ~ 610 cm^{-1} Raman modes, are seen. At $T=100$ K, the peaks at ~ 480 and ~ 610 cm^{-1} experience a sensible intensity increase, and a small diffusive contribution is observed [see Fig. 5(b)]. As the temperature further increases, the intensity of the high-frequency modes are reduced, and the diffusive contribution is enhanced. For $y=1.0$ [see Fig. 5(c)] and $T=10$ K, Raman peaks are observed at 90, 150, 220, 270, 305, 480, and 610 cm^{-1}. The splitting of the rotational modes observed between 200 and 300 cm^{-1} is probably caused by the large orthorhombic distortion found in this compound.[26] The Raman spectrum of this sample remain nearly unchanged as the temperature increases up to 100 K. For $T>100$ K, the diffusive contribution is enhanced, and the intensity of the high-frequency peaks is reduced.

IV. DISCUSSION

Our results will be discussed in the light of PS scenario for manganites with weak FM coupling.[7] The large thermal hysteresis observed in the magnetization curve of the $y=0.5$ sample for $H_{app}=1$ T [see Fig. 1(b)] actually suggests the coexistance of two phases. This was already observed in other reduced-T_C manganites.[7] For the $y=0.5$ sample and $H_{app}=5$ T, the AFM domains are *melted* (see Fig. 2), and the thermal hysteresis in the magnetization curve disappears [see Fig. 1(b)]. From Fig 2(a), at $T=2$ K, the AFM domains are estimated to correspond to $\sim 20\%$ of the sample volume before the application of an external field. After the application and release of a magnetic field of 5 T, the sample becomes entirely FM, indicating that the AFM domains are metastable at $T=2$ K. Differently, at $T=100$ K, the AFM domains that are *melted* for $H_{app}>1.5$ T [see Fig. 2(b)], are again present after the release of the magnetic field, indicating that the PS state is indeed the most stable configuration at this temperature and zero field.

It is intriguing that thermal hysteresis is not observed in the magnetization curves of our $Nd_{2/3}Ca_{1/3}MnO_3$ sample at any applied field [see Fig. 1(c)], despite the fact that PS may also be present in this sample, as suggested by the magnitude of the low-T magnetization. The slow increase in the magnetization of this sample, as the temperature decreases, may be described as a very smooth second-order-like transition between the AFM and FM states, which is not fully accomplished for any applied field in the studied range, even at low T.

A point that often arises in the study of doped manganites is the role of compositional inhomogeneities on the physical properties of these materials.[11,27] The rather broad FM transition in the low-field ($H_{app}=1$ T) magnetization curve for the $y=0.5$ compound [see Fig. 1(b)] was originally ascribed to a T_C distribution throughout the sample caused by fluctuations of the La/Nd ratio.[12] Nevertheless, for $H_{app}=5$ T, the shape of the magnetization curves for $y=0.0$ and $y=0.5$ are similar. Notice that, for $y=0.5$, the FM transition is broader for $H_{app}=1$ T than for $H_{app}=5$ T (see Fig. 1). Therefore, compositional fluctuations cannot alone account for the broadness of the low-field FM transition of the $y=0.5$ sample, and the FM and AFM domain structure may be responsible for it. For $y=0.5$ and $H_{app}=5$ T, the AFM domains *melt* into FM regions, and the shape of the magnetization curve near the transition is similar to that of the y

$=0.0$ sample [see Figs. 1(a) and 1(b)]. The similarity between both curves at $H_{app}=5$ T suggests that the $y=0.0$ and $y=0.5$ samples have equivalent distribution of cationic inhomogeneities.

It is interesting to mention that, although magnetization measurements indicate the presence of $\sim 20\%$ of AFM domains in the $y=0.5$ sample at low T, x-ray powder diffraction profiles show, within our experimental resolution, a single crystallographic phase for all studied samples (see Fig. 3). Notice that the $x=1/2$-type AFM phase[7] tends to show a large orthorhombic separation of the lattice constants (see inset of Fig. 3, and Refs. 4 and 18). Hence, the presence of $\sim 20\%$ of this phase for $y=0.5$ should be observable in our low T x-ray powder diffractograms. Notice that the T variation of the ''single-phase'' lattice parameters for $y=0.5$ show anomalies that seem to be correlated to the CO, AFM, and FM transitions [see Fig. 4(b)], which are supposed to take place at different regions of the sample. We believe that interface strains between the FM and AFM domains in this compound may decrease the orthorhombic distortion of the AFM (minority) phase, leading to the observation of only one crystallographic phase for the $y=0.5$ sample, within our experimental resolution.

Additional informations about the structure of the studied samples are obtained from our Raman-scattering measurements [see Figs. 5(a)–5(c)]. The high-frequency peaks (HFP) at ~ 480 and ~ 610 cm^{-1} are characteristic of manganites showing $x=0.0$ and $x=0.5$ types of Mn e_g orbital-ordered structures.[23] These features were also observed in doped samples in the PM phase,[21,22,28] and, more recently, in the charge-ordered $Pr_{0.65}Ca_{0.35}MnO_3$ compound.[29] Therefore, the observation of the HFP in the Raman spectra of manganites may be the signature for local and/or cooperative distortions of the $MnO_{6/2}$ octahedra. For the $(La_{1-y}Nd_y)_{2/3}Ca_{1/3}MnO_3$ sample with $y=0.5$, the weak HFP observed at $T=10$ K [see Fig. 5(b)] indicate the presence of a small fraction of CO and OO domains. These domains are possibly responsible for the low-T AFM component detected by our magnetization measurements. At $T=100$ K, the intensity of the HFP is substantially enhanced [see Fig. 5(b)], suggesting that the fraction of the CO and OO domains increase. This result is possibly related with the decrease of the FM component for this sample at $T\sim 100$ K [see Fig. 1(b)]. Finally, the weakening of the HFP for $T\gtrsim 150$ K for this sample [see Fig. 5(b)] may be associated to the gradual *melting* of CO and OO regions induced by thermal disorder. For the $y=1.0$ sample [see Fig. 5(c)], the temperature dependence of the HFP intensities at $T>100$ K are similar to that of the $y=0.5$ sample. Differently, at $T<100$ K, the HFP are much more intense for $y=1.0$ than for $y=0.5$ [see Figs. 5(b) and 5(c)], showing that the CO and OO domains are dominant in that sample even at low T. Again, this is consistent with the magnetization measurements, that shows that the low-T FM moment is small for $y=1.0$ [see Fig. 1(c)]. For $y=0.0$ [see Fig. 5(a)], contributions from the HFP are clearly identified only at temperatures near and above $T_C=265$ K, indicating a very small, if any, contribution from CO and OO domains at $T<200$ K for this sample. Finally, we should mention that all the samples show broad contribution from the HFP at $T=300$ K. This is likely related to short-range charge and orbital correlations, recently observed in the PM phase of optimally doped manganites.[30,31]

V. CONCLUSIONS

In summary, dc-magnetization, x-ray diffraction, and Raman-scattering measurements were performed in $(La_{1-y}Nd_y)_{2/3}Ca_{1/3}MnO_3$ ($y=0.0,0.5,1.0$) polycrystalline ceramic samples. Our results allow us to associate the presence of charge- and orbital-ordered domains (probed by Raman scattering) with the antiferromagnetic component of the spin system, determined by dc-magnetization measurements. Thus, this indicates that both phenomena are closely related. X-ray measurements for the $y=0.5$ sample show, within our experimental resolution, a single structural phase, with lattice parameter anomalies that may be associated with the various electronic and magnetic transitions observed in this material.

ACKNOWLEDGMENTS

This work was supported by FAPESP Grants No. 95/4721-4, 96/4625-8, 97/03065-1, and 97/11563-1 São Paulo-SP-Brazil.

*Present address: NIST Center for Neutron Research, National Institute of Standards and Technology, Gaithersburg, MD 20899 and Center for Superconductivity Research, Department of Physics, University of Maryland, College Park, MD 20742.

[1] E.O. Wollan and W.C. Koehler, Phys. Rev. **100**, 545 (1955).
[2] J.B. Goodenough, Phys. Rev. **100**, 564 (1955).
[3] C.H. Chen and S-W. Cheong, Phys. Rev. Lett. **76**, 4042 (1996).
[4] P.G. Radaelli, D.E. Cox, M. Marezio, S-W. Cheong, P.E. Schiffer, and A.P. Ramirez, Phys. Rev. Lett. **75**, 4488 (1995).
[5] H.Y. Hwang, S-W. Cheong, P.G. Radaelli, M. Marezio, and B. Batlogg, Phys. Rev. Lett. **75**, 914 (1995).
[6] J.M.D. Coey, M. Viret, L. Ranno, and K. Ounadjela, Phys. Rev. Lett. **75**, 3910 (1995).
[7] M. Uehara, S. Mori, C.H. Chen, and S.-W. Cheong, Nature (London) **399**, 560 (1999).
[8] A. Moreo, S. Yunoke, and E. Dagotto, Science **283**, 2034 (1999), and references therein.
[9] W. Archibald, J.-S. Zhou, and J.B. Goodenough, Phys. Rev. B **53**, 14 445 (1996).
[10] J.-S. Zhou, W. Archibald, and J.B. Goodenough, Nature (London) **381**, 770 (1996).
[11] G.H. Rao, J.R. Sun, J.K. Liang, W.Y. Zhou, and X.R. Cheng, Appl. Phys. Lett. **69**, 424 (1996).
[12] G.H. Rao, J.R. Sun, J.K. Liang, and W.Y. Zhou, Phys. Rev. B **55**, 3742 (1997).
[13] J.-S. Zhou and J.B. Goodenough, Phys. Rev. Lett. **80**, 2665 (1998).
[14] M.R. Ibarra, G.-m. Zhao, J.M. De Teresa, B. García-Landa, Z. Arnold, C. Marquina, P.A. Algarabel, H. Keller, and C. Ritter, Phys. Rev. B **57**, 7446 (1998).
[15] J. Baszynski, J. Kovac, A. Kowalczyk, J. Magn. Magn. Mater. **195**, 93 (1999).

[16] Y. Moritomo, Phys. Rev. B **60**, 10 374 (1999).
[17] R.A. Young, A. Sakthivel, T.S. Moss, and C.O. Paiva-Santos, J. Appl. Crystallogr. **28**, 366 (1995).
[18] P.G. Radaelli, D.E. Cox, M. Marezio, and S-W. Cheong, Phys. Rev. B **55**, 3015 (1997).
[19] Q. Huang, A. Santoro, J.W. Lynn, R.W. Erwin, J.A. Borches, J.L. Peng, K. Ghosh, and R.L. Greene, Phys. Rev. B **58**, 2684 (1998).
[20] J.C. Irwin, J. Chrzanowski, J.P. Franck, Phys. Rev. B **59**, 9362 (1999).
[21] M.V. Abrashev, V.G. Ivanov, M.N. Iliev, R.A. Chakalov, R.I. Chakalova, and C. Thomsen, Phys. Status Solidi B **215**, 631 (1999).
[22] E. Liarokapis, Th. Leventouri, D. Lampakis, D. Palles, J.J. Neumeier, and D.H. Goodwin, Phys. Rev. B **60**, 12 758 (1999).
[23] E. Granado, N.O. Moreno, A. García, J.A. Sanjurjo, C. Rettori, I. Torriani, S.B. Oseroff, J.J. Neumeier, K.J. McClellan, S.-W. Cheong, and Y. Tokura, Phys. Rev. B **58**, 11 435 (1998).
[24] S. Yoon, H.L. Liu, G. Schollerer, S.L. Cooper, P.D. Han, D.A. Payne, S.-W. Cheong, and Z. Fisk, Phys. Rev. B **58**, 2795 (1998).
[25] H.L. Liu, S. Yoon, S.L. Cooper, S-W. Cheong, P.D. Han, and D.A. Payne, Phys. Rev. B **58**, R10 115 (1998).
[26] K. Liu, X.W. Wu, K.H. Ahn, T. Sulchek, C.L. Chien, and J.Q. Xiao, Phys. Rev. B **54**, 3007 (1996).
[27] E. Granado, P.G. Pagliuso, J.A. Sanjurjo, C. Rettori, S.B. Oseroff, M.T. Causa, A. Butera, A. Caneiro, M. Tovar, J.J. Neumeier, K.J. McClellan, S-W. Cheong, Y. Tokura, R. Sanchez, J. Rivas, and S. Schultz, *Non-Crystalline and Nanoscale Materials*, edited by J. Rivas and M.A. López-Quintela (World Scientific, Singapore, 1998), pp. 105-115.
[28] E. Granado, J.A. Sanjurjo, C. Rettori, F. Prado, R.D. Sánchez, A. Caneiro, and S.B. Oseroff, Phys. Status Solidi B **220**, 609 (2000).
[29] V. Dediu, C. Ferdeghini, F.C. Matacotta, P. Nozar, and G. Ruani, Phys. Rev. Lett. **84**, 4489 (2000).
[30] C.P. Adams, J.W. Lynn, Y.M. Mukovskii, A.A. Arsenov, and D.A. Shulyatev, Phys. Rev. Lett. **85**, 3954 (2000).
[31] P. Dai, J.A. Fernandez-Baca, N. Wakabayashi, E.W. Plummer, Y. Tomioka, and Y. Tokura, Phys. Rev. Lett. **85**, 2553 (2000).